Thermal stability and crystallization kinetic of Se-Te-Ag glassy alloys and thick films for electronic devices

K. I. Hussain[a], A. Ashour[b], E. S. Yousef[c], E. R. Shaaban[b,d,*]
[a]*Department of Radiological Sciences, College of Applied Medical Sciences, King Khalid University, Abha 61421, Saudi Arabia.*
[b]*Physics Department, Faculty of Science, Islamic University of Madinah, Almadinah Al-Munawarah 42351, Saudi Arabia*
[c]*Physics Dep., Faculty of Science, King Khalid University, P. O. Box 9004, Abha, Saudi Arabia*
[d]*Department of Physics, Faculty of Science, Al-Azhar University, Assiut 71542, Egypt*

The present work has examined the thermal features of glassy chacogenide materials Se0.75-xTe0.25Agx (x = 0, 2, 4, 6, 8, 10 at %). The thermal stability of these compositions has been assessed under non-isothermal conditions using Differential Scanning Calorimetry (DSC), which has been used to find the glass transition temperature (Tg), the initial crystallization temperature (Tin), the temperature corresponding to the top of the crystallization rate (Tp), and the melting temperature (Tm). In addition, the kinetic parameter Kr(T) was given as an additional sign of thermal stability. Among these compositions, it was discovered that Se0.71Te0.25Ag0.04 had the best glass-forming ability and glass-thermal stability. The average coordination numbers of the considered samples have been discussed in relation to these results. Additionally, we measured the sheet resistivity, ρ, whose thickness is equivalent to 1000 nm at heating rate 5 K/min, in this work to study the crystallization kinetics of thick films of Se0.75-xTe0.25Agx (x = 0, 2, 4, 6, 8, 10 at %) in the temperature range of 300 to 625 K. This range was sufficient to draw attention to two substantial areas in the resistivity versus temperature curve, and the derivation of resistivity as a function of temperature established that the films under study only had one crystallization region.

Received November 2, 2023; Accepted January 10, 2024)

Keywords: Chalcogenide glass, Thermal stability, Crystallization kinetic, Thick films, Electric resistivity

1. Introduction

Chalcogenide glasses have played an important rule in recent technologies due to their interesting properties. K. Tanaka and K. Shimakawa [1] have summarized their applications as phase change memories (DVDs), x-ray medical image sensors, highly sensitive vidicons, holographic memories, nonlinear devices, solar cells, and ionic devices. Chalcogenide alloys have received abundant attention due to their potential in variety of optoelectronic technological applications. Se-Te compounds have a lot of curiosity compared with pure Selenium, due to their higher photosensitivity, hardness and crystallization temperature and smaller aging effects [2–5]. Chalcogenide glasses doped with transition metal ions, have gained special interest due to their various applications [6-10]. Since the doping element alters mechanical, electrical, thermophysical, optical and magnetic properties of the host material due to the electronic and structural change of the glass network [11-13]. Ag-doped chalcogenide glasses became very distinguished materials for further research concerning their properties, structure and preparation [14–19]. They have many applications in optoelectronics such as photo-doping, optical imaging, photo lithography and phase change optical recording [20–27]. The effect of Ag- doping to Se-Te alloys on their structural, optical, thermal, and electrical properties have been investigated by various workers [28-43].

* Corresponding author: esam_ramadan2008@yahoo.com
https://doi.org/10.15251/CL.2024.211.65

The crystallization kinetics, glass-forming ability (GFA), and thermal stability of the chalcogenide alloys have a vital role in many applications. Differential scanning calorimetry (DSC) is simple and sensitive technique used to study the crystallization kinetics for the chalcogenide glasses, under two methods (i) isothermal and (ii) non-isothermal method. The non-isothermal method has several advantages, and it is preferred over the isothermal method, since it quick and has wide temperature range.

In the current work, the thermal features of the $Se_{0.75-x}Te_{0.25}Ag_x$ (x = 0, 2, 4, 6, 8, 10 at. %) chalcogenide glassy materials are investigated using differential scanning calorimetry (DSC) under non -isothermally settings. The effect of Ag -doping to Se-Te alloys on glass transition T_g, activation energy of glass transition E_g, activation energy of crystallization E_p, thermal stability and glass forming ability have been clarified in terms of the average coordination number. Also, the sheet resistance-temperature dependence of the $As_{40}S_{60-x}Se_x$ thick films with ($0 \leq x \geq 60$) at. %) are investigated. Then, we made us in mind that we can achieve and calculate the thermal crystallization kinetics of $As_{40}S_{60-x}Se_x$ thick films at heating rate equal to 5 K/min by calculating their resistivity as a function of temperature. The crystallized phases were confirmed over the temperature that realistic to the films by the technology of XRD.

2. Theoretical basis

2.1. Thermal stability parameters in terms of characteristic temperature.

Many criteria of thermal stability have been introduced, in correlation with the characteristic temperatures as the glass transition temperature, T_g, the initial crystallization temperature, T_{in}, the temperature corresponding to the top of crystallization rate, T_p, and the melting temperature, T_m. Dietzel defined an important glass thermal stability criterion [44],

$$\Delta T = T_{in} - T_g \tag{1}$$

The H_r criterion proposed by Hurby,

$$H_r = \Delta T / (T_m - T_{in}) \tag{2}$$

As a benefit of H_r criterion, two other criteria have obtained by Saad and Poulain, weighted thermal stability, H' and S criterion [45],

$$H' = \Delta T / T_g \quad \& \quad S = \left(T_p - T_{in}\right) \Delta T / T_g \tag{3}$$

The ability of glass formation k_{gl} is given by

$$k_{gl} = \frac{\left(T_{in} - T_g\right)}{\left(T_m - T_g\right)} \tag{4}$$

For specification the glass thermal stability, k_{gl} is more appropriate than ΔT.

2.1. Thermal stability in terms of kinetic parameters

According to the formal theory of transformation kinetics, crystallization rate is given by [46]:

$$\frac{d\chi}{dt} = n\left(1-\chi\right) I_1^{n-1} K_0 \exp\left(\frac{-E_c}{RT}\right) = nK\left(1-\chi\right) I_1^{n-1} \tag{5}$$

Here E_c is the activation energy for crystal growth and K is the reaction rate constant that shows Arrhenian temperature dependence throughout the formula:

$$K\left(T\right) = K_0 \exp\left(-\frac{E_c}{RT}\right) \tag{6}$$

$K(T_g)$ and $K(T_p)$ criteria have been proposed according to the literatures [47, 48]

$$K\left(T_g\right) = K_0 \exp\left(-\frac{E_c}{RT_g}\right) \tag{7-a}$$

And

$$K\left(T_p\right) = K_0 \exp\left(-\frac{E_c}{RT_p}\right) \tag{7-b}$$

where, these two criteria refer to the ability of glass devirtrification on heating. Here another stability criterion which is defined as

$$K_r\left(T\right) = K_0 \exp\left(-\frac{H_r E_c}{RT}\right) \tag{8}$$

where T is any temperature lies between T_g and T_p.

The smaller $K_r(T)$ values, the greater is the glass thermal stability. This method can specify the glass stability over a wide temperature range other than at only one temperature as T_g or T_p.

3. Experimental procedures

The bulk glass samples with composition $Se_{0.75-x}Te_{0.25}Ag_x$ (x = 0, 2, 4, 6, 8, 10 at %) were synthesized using melt-quenching technique. The preparation of the glass samples was presented in detailed elsewhere [9, 10]. X-ray powder diffraction (XRD) Philips diffractometry (1710) with Cu–Kα1 radiation have been used to investigate the non -crystalline structure of the different bulk glass samples. Energy Dispersive Analysis of X-rays (EDAX) has been used for the elemental analysis of investigated samples. Differential scanning calorimeter (DSC Shimadzu 50) was used to characterize the crystallization behavior for the glass samples at various heating rates between 5 and 40 K/min under non-isothermal conditions. The experimental setting and conditions of DSC Shimadzu 50 was presented elsewhere [10]. The glass transition temperature, T_g, the initial crystallization temperature, T_{in}, the temperature corresponding to the top of crystallization rate, T_p, and the melting temperature, T_m were determined. Thermal evaporation technique was used to prepare the thick films. The as-prepared films were uniform, pinhole free and strongly adherent to the glass substrates. The layer thickness of thin films was measured by using a quartz crystal monitor (Edwards model FTMS). The thickness of thin films in all samples found to equal to 1000 nm with an accuracy of 10%. A digital picoammeter (DPM-111 Scientific Instruments, Roorkee) and two-point probe method used to record the resistivity, R_s of the investigated samples in the temperature range 300 to 435 K. The structural analyses of such films were done by Philips x-ray diffractometer (model-x ′ pert) with Cu-K_α radiation (λ = 1.54056 Å). The data was collected by step-scan modes in 2θ range between 5-10° and 70° with step-size of 0.02° and step time of 0.6 seconds.

4. Results and discussion

Fig. 1 shows XRD pattern of $Se_{0.75-x}Te_{0.25}Ag_x$ (x = 0, 6, 10 at. %) chalcogenide glasses, the broad humps confirm the non crystalline nature of these compositions. The two broad peaks inform about the existence of two amorphous phases in all these compositions. EDAX of $Se_{0.75}Te_{0.25}$ and $Se_{0.69}Te_{0.25}Ag_{0.06}$ compositions are shown by figures 2.a and 2.b, these figures confirm the adequate ratio of the involved elements with an experimental error does not exceed ±1%. The EDXS analyses shows that the grown compositions were closely stoichiometric.

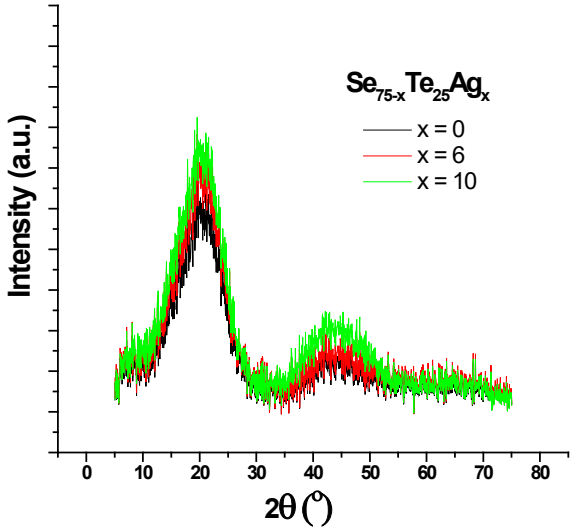

Fig. 1. X-ray diffraction patterns of Se_{75-x}-Te_{25}-Ag_x (x = 0, 2, 4, 6, 8, 10 at %) compositions.

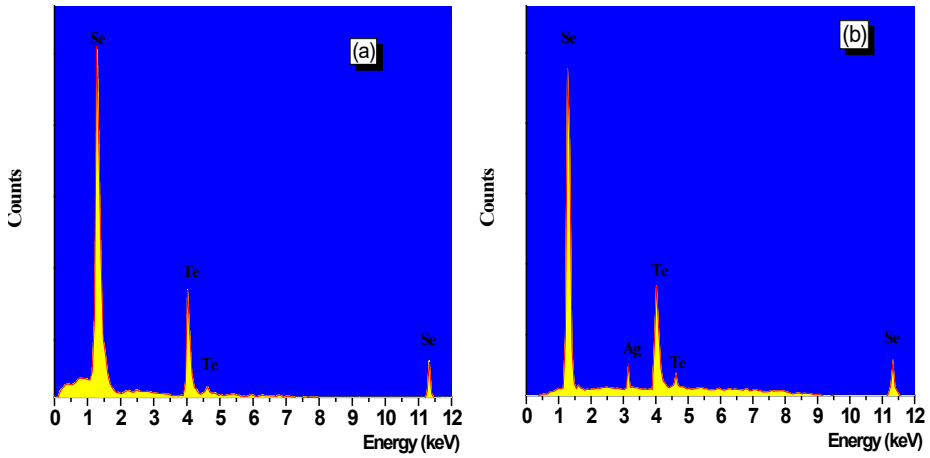

Fig. 2. (a, b) The energy dispersive X-ray spectrum (EDXS) of Se_{75-x}-Te_{25}-Ag_x (x = 0 and 6 at % respectively) chalcogenide glasses.

The thermal characteristics of $Se_{0.75-x}Te_{0.25}Ag_x$ (x = 0, 2, 4, 6, 8, 10 at. %) chalcogenide glasses were achieved using DSC experimental procedures at heating rates between 5 and 40 K/min. For simplicity, we have pointed to $Se_{0.75-x}Te_{0.25}Ag_x$ (x = 0, 0.02, 0.04, 0.06, 0.08, 0.1) compositions as abbreviation codes from Y1 to Y6, with the variation of Ag- doping content from 0 to 0.1 respectively.

Figure 3 shows the typical DSC traces for the as prepared $Se_{0.69}Te_{0.25}Ag_{0.06}$ composition at heating rates (β = 5 - 40 K/min). Four characteristic temperatures can obviously be shown; the glass transition temperature (T_g), the onset temperature of crystallization (T_c), the crystallization

peak temperature (T_p)and the melting temperature (T_m). Estimated values of these characteristic temperatures are shown in table.1. In chalcogenide glasses the glass transition temperature (T_g) is very important, since the glass transition nature is very complicated and still poorly to understood. From table 1 it can be shown that T_g increases with increasing heating rates for all the glass samples under investigation. With increasing Ag content, the T_g shows two different trends. For samples (Y1 - Y3), the T_g value decrease with increasing Ag-content, while for samples (Y4 - Y6) it increases with increasing Ag-content at different heating rates, this will be discussed later in accordance with the average coordination number.

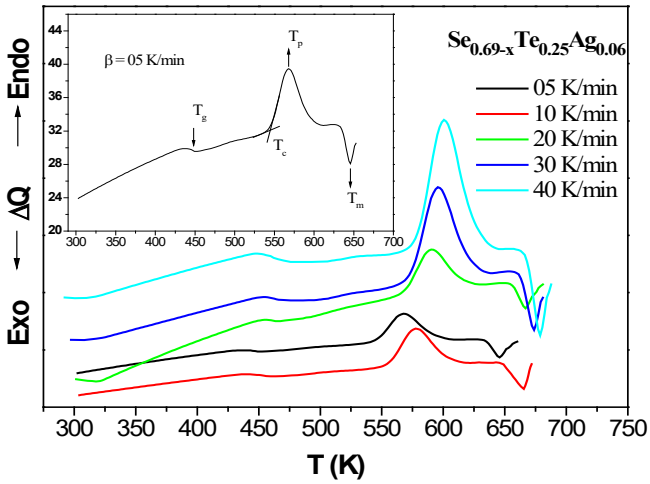

Fig. 3. The DSC traces of the as prepared $Se_{0.69}$-$Te_{0.25}$-$Ag_{0.06}$ compositions at different heating rates (β = 5, 10, 20, 30, 40 K/min).

Table 1. The values of thermal parameters of glass transition temperature T_g, onset temperature of crystallization T_{in}, crystallization temperature T_p and melting temperature T_m of $Se_{75-x}Te_{25}Ag_x$ ($0 \le x \le 10$) alloys with different heating rates β. The characteristic parameters, ΔT, H_r, H' and S are according to the text.

Alloy	β	T_g (K)	T_{in}(K)	T_{in}(K)	T_p(K)	ΔT(K)	H_r	H'	S(K)
Y1	5	439.7	532.4	548	648	92.63	0.926	0.211	3.286
	10	446.6	541.1	557.7	663	94.58	0.898	0.212	
	20	454.4	550.9	568.4	679	96.53	0.873	0.212	
	30	460.2	556.7	575.3	690	96.53	0.841	0.21	
	40	464.1	561.6	580.1	697	97.5	0.834	0.21	
Y2	5	436.7	535.4	552	645.1	98.63	1.059	0.226	3.749
	10	443.6	544.1	561.7	660.1	100.6	1.023	0.227	
	20	451.4	553.9	572.4	676.1	102.5	0.989	0.227	
	30	457.2	559.7	579.3	687.1	102.5	0.951	0.224	
	40	461.1	564.6	584.1	694.1	103.5	0.941	0.224	
Y3	5	431.7	537.4	554	643.1	105.6	1.185	0.245	4.061
	10	438.6	546.1	563.7	658.1	107.6	1.14	0.245	
	20	446.4	555.9	574.4	674.1	109.5	1.099	0.245	
	30	452.2	561.7	581.3	685.1	109.5	1.055	0.242	
	40	456.1	566.6	586.1	692.1	110.5	1.043	0.242	
Y4	5	441.7	530.4	550	650	88.63	0.886	0.201	3.932
	10	448.6	539.1	559.7	665	90.58	0.86	0.202	
	20	456.4	548.9	570.4	681	92.53	0.837	0.203	
	30	462.2	554.7	577.3	692	92.53	0.807	0.200	
	40	466.1	559.6	582.1	699	93.5	0.8	0.201	
Y5	5	443.7	528.4	546	651.9	84.63	0.799	0.191	3.357
	10	450.6	537.1	555.7	666.9	86.58	0.778	0.192	
	20	458.4	546.9	566.4	682.9	88.53	0.76	0.193	
	30	464.2	552.7	573.3	693.9	88.53	0.734	0.191	
	40	468.1	557.6	578.1	700.9	89.5	0.729	0.191	
Y6	5	445.7	525.4	544	654.9	79.63	0.718	0.179	3.323
	10	452.6	534.1	553.7	669.9	81.58	0.702	0.180	
	20	460.4	543.9	564.4	685.9	83.53	0.688	0.181	
	30	466.2	549.7	571.3	696.9	83.53	0.665	0.179	
	40	470.1	554.6	576.1	703.9	84.5	0.662	0.180	

4.1. Activation energies for glass transition E_g and for crystallization kinetic E_c

The activation energies of glass transition were determined using Kissinger relation, [49] which given by:

$$\ln\left(\frac{T_g^{\,2}}{\beta}\right) = \frac{E_g}{RT_g} + const \tag{9}$$

Here R is the universal gas constant.

Fig. 4 illustrate the relation between $\ln\left(\frac{T_g^2}{\beta}\right)$ versus ($1/T_g$), which was found to be a straight line, the E_g value calculated from the slope of the straight line corresponding to each sample. The variation of E_g with different Ag- doping content can be shown in Fig .5. It is obviously shown that E_g has two different behaviors; for samples (Y1 - Y3) E_g decreases with increasing Ag content, while for samples (Y4- Y6) it increases with Ag content, which is the same manner of T_g variation.

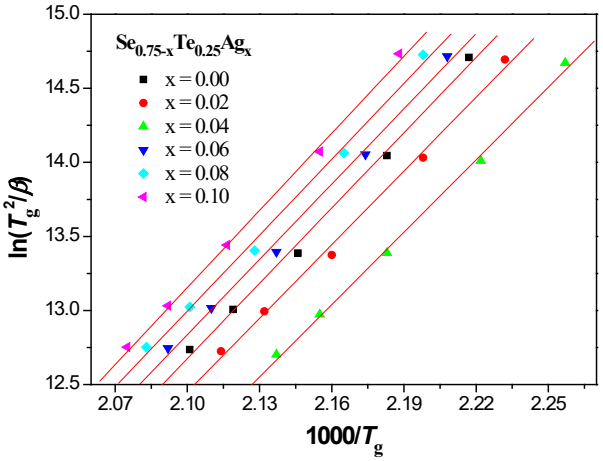

Fig. 4. Plots of $\ln\left(\frac{T_g^2}{\beta}\right)$ *versus (1/*T_g*) of* Se_{75-x}*-*Te_{25}*-*Ag_x *(x = 0, 2, 4, 6, 8, 10 at %) glassy alloys and straight regression lines for all these alloys.*

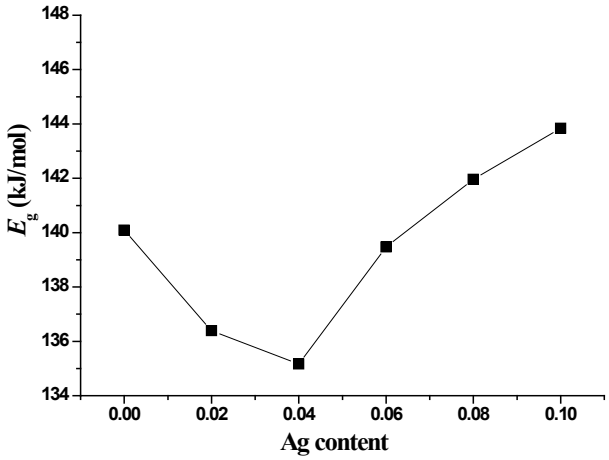

Fig. 5. Variation of activation energy of glass transition E_g *versus Ag doping ratio in* Se_{75-x}*-*Te_{25}*-*Ag_x *(x = 0, 2, 4, 6, 8, 10 at %) glasses.*

The activation energy E_g is defined as the needed energy by atoms groups in glass transition state to bound between two possible metastable states. Based on this definition, the atoms groups in a system with the lowest activation energies have the largest possibility to bound to a metastable state with lowest internal energy. $Se_{0.71}Te_{0.25}Ag_{0.04}$ glass has the minimum value of E_g, hence it has a larger possibility to bound to a lower configurational energy state.

To estimate the activation energy of crystallization (E_c), Kissinger relation [49] which modified by Vazquez et al [50] for non-isothermal analysis were used as following:

$$\ln\left(\frac{T_p^2}{\beta}\right)=\frac{E_c}{RT_p}+\ln\left(\frac{E_c}{RK_0}\right) \tag{10}$$

K_o is a factor inform about effective molecular collisions probability of the formation of the activated complexes in each case.

Fig. 6 depicted $\ln\left(\frac{T_p^2}{\beta}\right)$ versus $1/T_p$ plot for different compositions, the activation energy, E_c and the frequency factor, K_o are then obtained. The factor K_0 are calculated from the intercept of the straight line with the vertical axis Fig.7 illustrate the variation of E_c and K_o as a function of Ag doping content. E_c and K_o are increase in (Y1- Y3) samples with increasing Ag content, then they decrease for sample (Y4 -Y6) with Ag content.

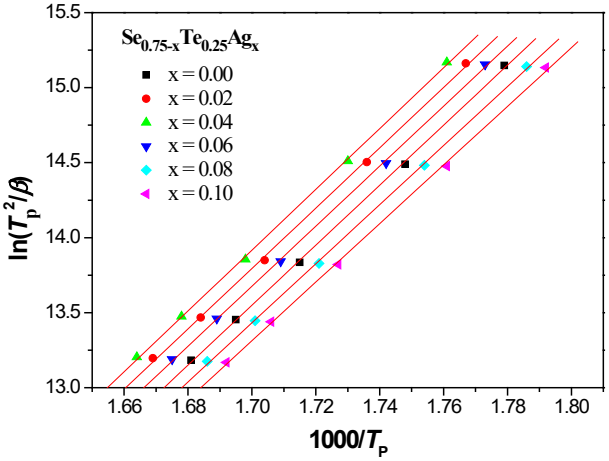

Fig. 6. Plots of $\ln\left(\frac{T_p^2}{\beta}\right)$ *versus* $(1/T_p)$ *of* Se_{75-x}-Te_{25}-Ag_x *(x = 0, 2, 4, 6, 8, 10 at %) chalcogenide glasses and straight regression lines for all these alloys.*

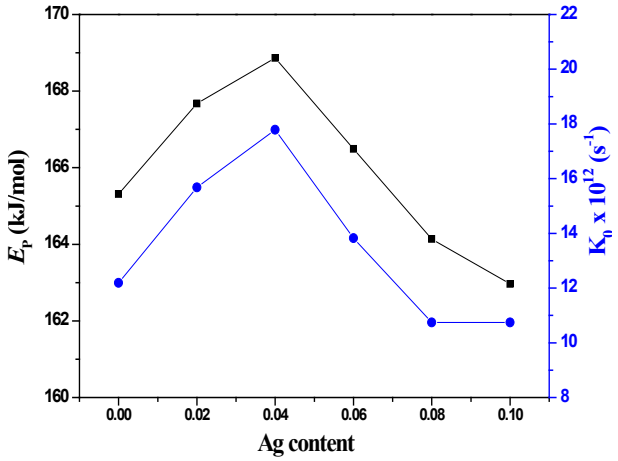

Fig. 7. The values of the activation energies E_c *and the frequency factors* K_o *as a function of Ag content.*

4.2. Thermal stability glassy Se-Te-Ag glassy alloys

In various technological applications, it is important for the chalcogenide material to be good glass former and thermally stable. As discussed above in the theoretical parts, the thermal stability criteria and the glass forming tendency can be evaluated using the characteristic temperatures T_g, T_{in}, T_p, and T_m given in table.1. It is clear from figure 8 that the glass forming

tendency k_{gl} decreases slowly with increasing the heating rate for all the glass samples. On the other hand, k_{gl} gives unstable manner with the variation of Ag content. The glass sample of Ag-doping ratio 0.04, 0.02, 0.06 (Y3, Y2 and Y4 glass) have the greatest values of k_{gl} respectively, while the specimens of Ag -doping content 0.1, 0.8 and 0.0 (Y6, Y5 and Y1 glass) have the lowest k_{gl} values respectively.

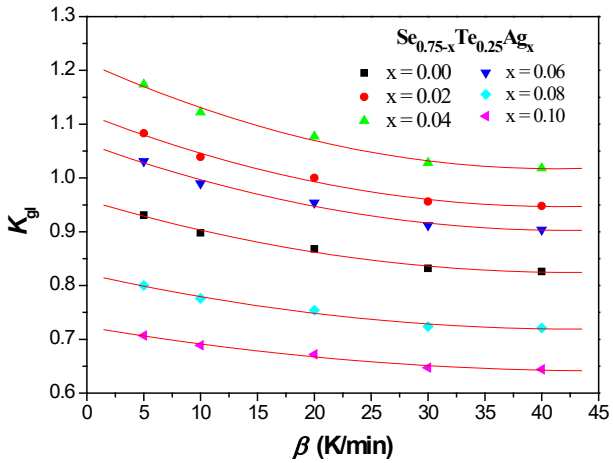

Fig. 8. The glass forming ability k_{gl} against heating rates for various composition of Se_{75-x}-Te_{25}-Ag_x (x = 0, 2, 4, 6, 8, 10 at %) glasses.

The H_r which is an important indicator for the glass forming ability (GFA) also was shown in table 1. It can be shown that H_r decrease with increasing heating rate for all glass samples. While it increases with further addition of Ag in Y1, Y2 and Y3 samples and decreases with increasing Ag doping rate in Y4, Y5 and Y6 samples. From table 1, it is also can be observed that $H^{/}$ and S(k) criteria have the same manner of variation with increasing Ag content within these compositions. Thus, we can concluded that Y3 sample (Ag doping rate = 0.04) has the highest glass forming ability and glass thermal stability between these compositions.

K(T) and $K_r(T)$ parameters of studied alloys were calculated by using: Eqs. 7 (a, b) and 8, respectively. These calculations were compared with those obtained from stability criteria based on characteristic temperatures. Fig. 9 (a, b) show plotting of $K_r(T)$ versus T at two different heating rates β = 30 K/min and β = 10 K/min respectively. It was shown that $K_r(T)$ decreases with increasing Ag content for (Y1 - Y3) samples over the entire temperature range, which indicate a high thermal stability for the (Y3) sample. Also, it can be shown that $K_r(T)$ increases with increasing Ag content from 0.06 to 0.1 over the entire temperature range, which means that the thermal stability decreases with increasing Ag doping level. Hence these results confirm the above-mentioned results of thermal stability achieved by $H^{/}$, H_r and S criteria based on characteristic temperatures T_g, T_{in}, T_p, T_p (table.1).

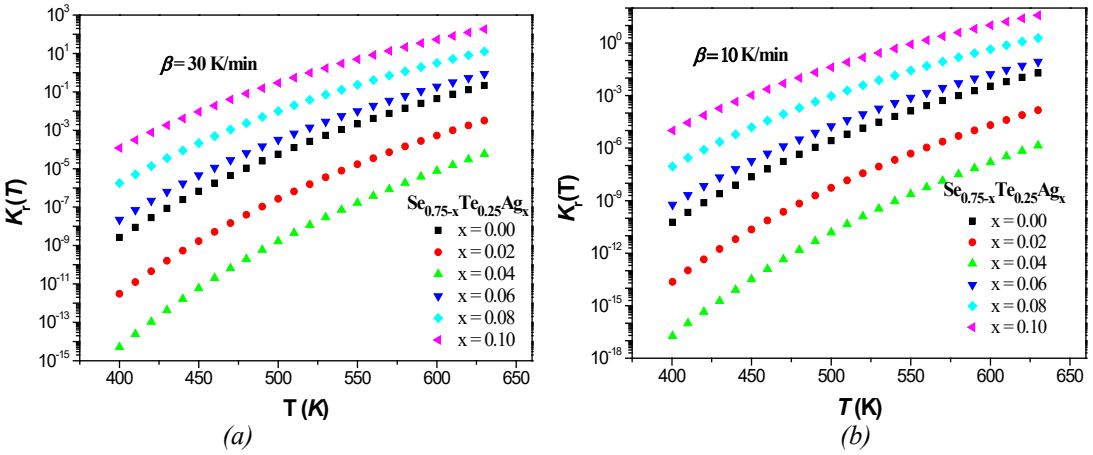

Fig. 9 (a) Plots of $K_r(T)$ versus T of Se_{75-x}-Te_{25}-Ag_x (x = 0, 2, 4, 6, 8, 10 at %) glasses at β = 30 K/min; (b) Plots of $K_r(T)$ versus T of Se_{75-x}-Te_{25}-Ag_x (x = 0, 2, 4, 6, 8, 10 at %) glasses at β = 10 K/min.

The $K_r(T)$ values for the temperatures T_g and T_p are obtained using the relation given by eq. 8. Fig. 10 and Fig. 11 represent the variation of $K_r(T_g)$ and $K_r(T_p)$ with heating rates for all the compositions under investigation respectively. $K_r(T_g)$ and $K_r(T_p)$ show the same behavior as $K_r(T)$, which emphasize the same results of thermal stability of these compositions.

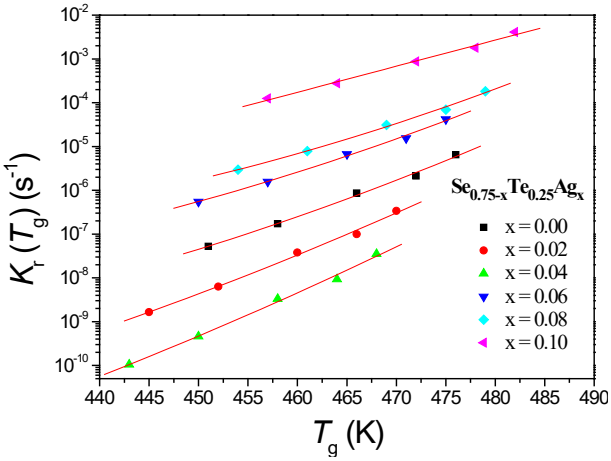

Fig. 10. The variation of $K_r(T_g)$ with heating rates for Se_{75-x}-Te_{25}-Ag_x (x = 0, 2, 4, 6, 8, 10 at %) glassy compounds.

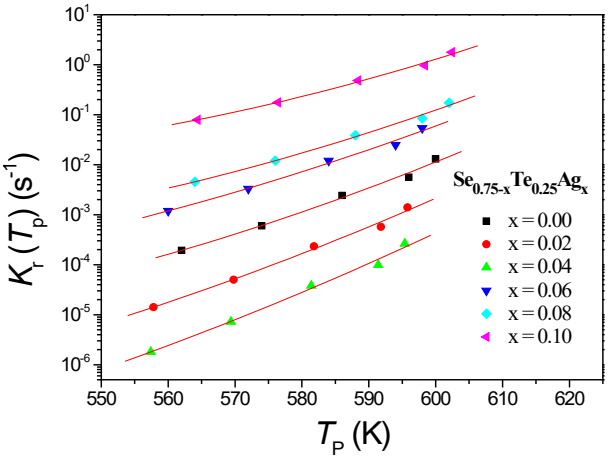

Fig. 11. The variation of $K_r(T_p)$ with heating rates for Se_{75-x}-Te_{25}-Ag_x (x = 0, 2, 4, 6, 8, 10 at %) glassy compounds.

The average coordination number, *CN*, the average heat of atomization H_{av} , single bond strength S_{bt} and the numbers of lone pairs electrons L of Se_x-Te_y-Ag_z ternary compound ($x + y + z = 1$) have been calculated according to the literature [10], their values are listed in table 2. The bond energies have been calculated in view of the chemical bond approach which have been discussed in detail in many works [9, 10]. Se-Te bonds (43.34 kcal/ mol), Se-Ag (41.5 kcal/mol) and bonds are expected to occur in the system under investigation. After the formation of these bonds, unsatisfied Se valences are much satisfied by the formation of Se–Se bonds (43.81 kcal/mol). The number of excess homopolar bonds for each composition of the Se_{75-x}-Te_{25}-Ag_x (x = 0, 2, 4, 6, 10 at. %) are listed in table.2. Knowing the bond energies, the cohesive energy (*CE*) has been derived [9, 10] and listed in table 2. These results may be due to the decrease of the relative atomic mass of chalcogen (Se) or its proportion in a chalcogenide glass system, which increases the average bond strength [9, 10]. It is worth to note that the average coordination number in the investigated compositions varies from 2 to 2.5 as Ag content varies between 0.0 and 0.1; hence the deduced glass thermal stability may be discussed in terms of the topological model [51]. Based on this model, the glass has it most stability at an average coordination number CN = 2.4, hence the glass network has a mechanical threshold at which it turns from a floppy glass to more rigid glass. It was assumed that the atomic interactions are only a covalent type. Chalcogenides doped with Ag have ionic conduction [52], which refers to the existence of ionic bonds. The physical properties of glass are affected by the metallic properties [53] and the threshold of CN = 2.4 may be shifted to about 2.3. In our system under study $Se_{0.75-x}Te_{0.25}Ag_x$ (x = 0, 2, 4, 6, 8, 10 at. %), the average coordination number values are 2, 2.1, 2.2, 2.3, 2.4, 2.5 for Ag doping ratio = 0, 2, 4, 6, 8 and 10 at. % respectively. It is obvious that the turning point between the polymeric glass to a more rigid glass occurred at CN = 2.2 (Y3; the sample with 4 at % Ag doping has the higher thermal stability) i.e that at an average coordination number less than 2.3. The average coordination number value expresses the maximum at which the transformation happens from the under constrained polymeric network to the over constrained rigid network, which give the network its extreme thermal stability. We agree to some where with a previous work have done by M.A. Abdel-Rahim et al [32], they have investigated the thermal properties in $Se_{90-x}Te_{10}Ag_x$ (x = 4, 6, 8 at. %) compositions and the transformation from the floppy state to the rigid one has occurred at an average coordination number CN = 2.3.

Table 2. The average coordination number CN, the average heat of atomization H_{av}, the cohesive energy CE, numbers of lone pairs electrons L, S_{bt} single bond strength and excess of homopolar bonds E_x as a function of Ag content of the $Se_{75-x}Te_{25}Ag_x$ ($0 \le x \le 10$) glassy compositions.

Ag	Sample	CN	H_{ss}	S_{bt}	L	CE	E_x
0	Y1	2	48.55	24.275	4	1.889	100
0.02	Y2	2.1	48.922	24.708	4.04	1.868	94
0.04	Y3	2.2	49.294	25.15	4.08	1.847	88
0.06	Y4	2.3	49.666	25.601	4.12	1.826	82
0.08	Y5	2.4	50.038	26.061	4.16	1.805	76
0.1	Y6	2.5	50.41	26.532	4.2	1.784	70

4.3. Crystallization kinetics of $Se_{90-x}Te_{10}Ag_x$ films in terms of resistivity measurements

The experimental relationship between resisstivity, ρ with temperature of c $Se_{90-x}Te_{10}Ag_x$ films (1000 nm) at heating rate 5 K/min is presented in Fig. 12 (a). These measurements of the heat treatment films were performed to determine thermal properties based on electrical measurements. Fig. 12 (b) shows the ρ decreases continuously until an abrupt drop shows at a certain temperature for corresponding studied samples and these temperature are called the intial crystallization temperature, T_{in}, this gradient continues until it gets to the highest degree of crystallization, T_p and then the sheet resistance decreases in a continuous behavior after that. In the

range (RT-640 K), the arrangement of atoms is not clearly changed with temperature, and therefore, the ρ decreases gradually in this temperature range but slowly. In this region, the state of the studied films is amorphous and the arrangement of atoms is random, causing its high ρ. When the temperature is increased above T_{in}, the atoms have sufficient energy to rearrange. The arrangement of atoms is ordered such that the films are transformed from amorphous to crystalline state and the ρ rapidly decrease. This is due to the grain growth of the film proceeding as the temperature is increased [17].

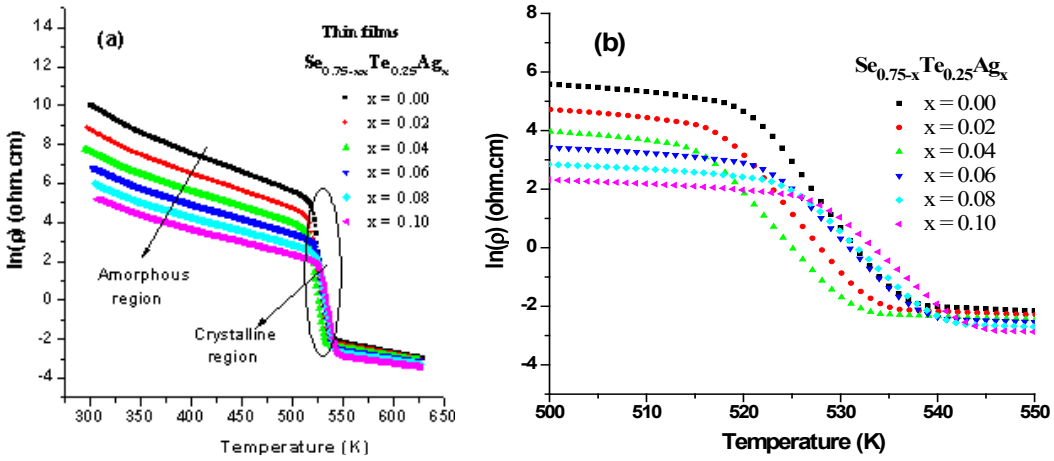

Fig. 12 (a) Variation of resistivity ρ versus temperature of Se_{75-x}-Te_{25}-Ag_x (x = 0, 2, 4, 6, 8, 10 at %) glassy compounds; (b) magnified plot of resistivity ρ of Se_{75-x}-Te_{25}-Ag_x (x = 0, 2, 4, 6, 8, 10 at %) glasses in temperature range (630-700 K).

On the other hand, the derivation of resistivity, ρ from the first degree relative to the temperature will lead us to know the first pillar of thermal studies. Fig. 13 appears the relationship between the derivative of sheet resistance, $d\rho/dT$ and temperature, T. Now, the exothermic heat flow is given by the following equation:

$$\Delta Q_{exo} = -[\frac{d\rho}{dT}]_{exo}$$

Resistance measurements are now being made with temperature at different heating rates to determine the activation energy of the crystalline films and the crystallization mechanism for such films.

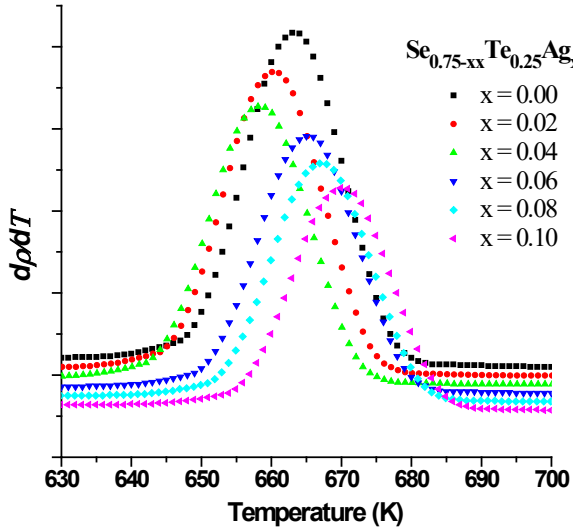

Fig. 13. The calculated exothermic heat flow ΔQ_{exo} = - dρ/dT and Temperature T of Se_{75-x}-Te_{25}-Ag_x (x = 0, 2, 4, 6, 8, 10 at %) glasses.

4.4. Crystalline phases of annealed Se-Te-Ag glass utilizing XRD

The XRD patterns of $Se_{0.75-x}Te_{0.25}Ag_x$ (x = 0, 0.06, 0.1) alloys annealed beyond the top temperature of crystallization with a heating rate of 5 K min^{-1} for 2 h are presented in Fig. (17). The diffractograms of the transformed material after the crystallization progression propose the occurrence of microcrystallites, from the JCPDS files these peaks can be recognized as two phase of binary Se-Te (card no.1-87-2413) and Se-Ag (card no.3-65-2878), While there are still more amorphous stages, which are illustrated by the final two large humps in Fig. 14. Since there are changes in intensity between each phase's prominent peak, the identical crystalline phases could be recognized in all the samples. As mentioned before, the addition of Ag concentrations over the threshold structure reducing the Se-Ag bonds and increasing the strength of the Ag-Ag bonds in glassy form which effect on dangling bonds and defects. The X-ray diffraction pattern of $Se_{0.75-x}Te_{0.25}Ag_x$ films studies indicate that the crystallization reaction for the film corresponds to the formation of major crystallize phase from Se-Te and a small trace from Se-Ag. Also, it is found that E_c of $Se_{0.75-x}Te_{0.25}Ag_x$ glasses increases progressively with Ag content reaching to its maximum value at Ag = 0.04 and then decreases. This may be attributed to the appearance of Se-Ag traces with reduced bonds compared to Ag-Ag bonds which does not appear in the crystalline phases, also may be produced by the increased density of defects and dangling bonds in the sample Y3 (Ag = 0.04), hence a portion of the energy required in crystal formation is used to minimize defects and dangling bonds.

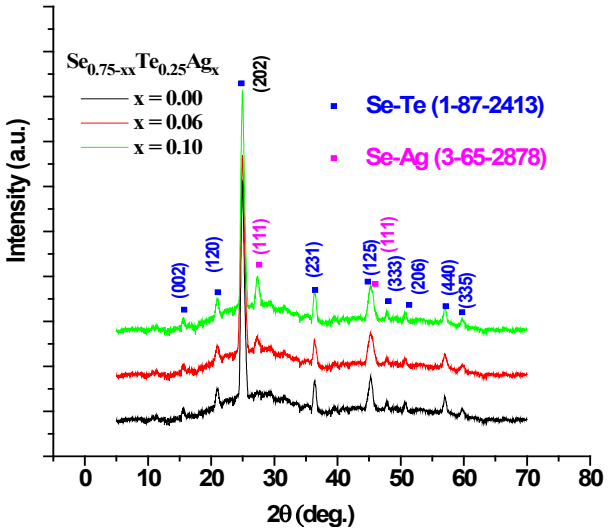

Fig. 14. The X-ray diffraction patterns of crystallized Se_{75-x}-Te_{25}-Ag_x alloys.

5. Conclusion

A calorimetric analysis according to non-isothermal specifications presented to investigate the thermal characteristic of the $Se_{0.75-x}Te_{0.25}Ag_x$ ($0 \leq x \leq 0.1$) glasses. The thermal findings estimated by several criteria as H_r, $H^{\backslash}$, S and k_{gl} that is founded upon the distinctive temperatures T_g, T_{in}, T_p, T_m, as viewed in this research, imply that $Se_{0.71}Te_{0.25}Ag_{0.04}$ composition have a superior thermal stability and a greater glass forming ability. The K_r criterion which is associated to the activation energy of crystallization has highlighted the same findings of stability of the studied glasses. These findings have been explained in terms of the average coordination number values which express the maximum at which the transformation happens from the under constrained polymeric network to the over constrained rigid network. Also, the crystallization kinetic of $Se_{0.75-x}Te_{0.25}Ag_x$ thick films via measuring the sheet resistance, R_s and by means of the derivation of sheet resistance with regards to temperature, the exothermic crystallization peaks was deduced. According to the understanding of the crystallization kinetics in these alloys, we recommend the development of these alloys for technological applications established on the amorphous to crystallization phase variation.

Acknowledgments

The authors extend their appreciation to the Deanship of Scientific Research at King Khalid University for funding this work through the research group program under grant number (RGP.2/583/44)

References

[1] Tanaka, K. and K. Shimakawa, Amorphous Chalcogenide Semiconductors and Related Materials. 2011: Springer New York; https://doi.org/10.1007/978-1-4419-9510-0

[2] Majeed Khan, M., et al., Journal of Modern Optics, 2003. 50(2): p. 251-263; https://doi.org/10.1080/09500340210141172

[3] Bureau, B., et al., Molecules, 2009. 14(11): p. 4337-4350; https://doi.org/10.3390/molecules14114337

[4] Sharma, N. and S. Kumar, Turkish Journal of Physics, 2007. 31(3): p. 161-167.

[5] Bhargava, A., et al., Journal of non-crystalline solids, 1995. 192: p. 494-497; https://doi.org/10.1016/0022-3093(95)00397-5

[6] Balcerek, K., et al., Cryogenics, 1998. 38(12): p. 1233-1236; https://doi.org/10.1016/S0011-2275(98)00113-1

[7] Horigane, K., H. Hiraka, and K. Ohoyama, Journal of the Physical Society of Japan, 2009. 78(7): p. 074718-074718; https://doi.org/10.1143/JPSJ.78.074718

[8] Kumar, A., A. Sharma, N. Mehta, Progress in Natural Science: Materials International, 2019. 29(5): p. 541-548; https://doi.org/10.1016/j.pnsc.2019.09.004

[9] Soraya, M., Applied Physics A, 2020. 126(8): p. 1-9; https://doi.org/10.1007/s00339-020-03781-2

[10] Soraya, M., et al., Applied Physics A, 2018. 124(2): p. 1-11; https://doi.org/10.1007/s00339-018-1603-8

[11] Iovu, S., M. et al., J. Optoelectron. Adv. M., 2001. 3(2): p. 443-454. https://doi.org/10.1117/12.475321

[12] Trnovcova, V. et.al., J.Non-Cryst. Solids, 2007. 353: p. 1311-1314; https://doi.org/10.1016/j.jnoncrysol.2006.09.049

[13] Gubanova, A. et.al., Mold. J. of Phys. Sci., 2009. 8 (2): p. 178-185.

[14] Al-Ghamdi, A.A., Vacuum, 2006. 80(5): p. 400-405; https://doi.org/10.1016/j.vacuum.2005.07.003

[15] Tanaka, K., Journal of non-crystalline solids, 1993. 164: p. 1179-1182; https://doi.org/10.1016/0022-3093(93)91210-T

[16] Wagner, T., et al., International Journal of Electronics, 1994. 77(2): p. 185-191; https://doi.org/10.1080/00207219408926046

[17] Tanaka, K., et al., Journal of applied physics, 1995. 78(6): p. 3895-3901; https://doi.org/10.1063/1.359906

[18] Kawaguchi, T., S. Maruno, S.R. Elliott, Journal of Applied Physics, 1996. 79(12): p. 9096-9104; https://doi.org/10.1063/1.362644

[19] Ohta, M., Physica Status Solidi, 1997. 159(2): p. 461-468; https://doi.org/10.1002/1521-396X(199702)159:2<461::AID-PSSA461>3.0.CO;2-W

[20] Wágner, T., M. Frumar, V. ŠuškováJournal of non-crystalline solids, 1991. 128(2): p. 197-207; https://doi.org/10.1016/0022-3093(91)90514-7

[21] Wagner, T., Journal of Optoelectronics and Advanced Materials, 2002. 4(3): p. 717-727.

[22] Ramesh, K., et al., Journal of Physics Chemistry of Solids, 2000. 61(1): p. 95-101; https://doi.org/10.1016/S0022-3697(99)00239-5

[23] Frumar, M., et al., Photoinduced Changes of Structure and Properties of Amorpous Binary and Ternary Chalcogenides. 2001, Pardubice Univ (Czechoslovakia).

[24] Zhou, G.-F., Materials Science Engineering: A, 2001. 304: p. 73-80; https://doi.org/10.1016/S0921-5093(00)01448-9

[25] Chou, L.-H., et al., Japanese Journal of Applied Physics, 2001. 40(8R): p. 4924; https://doi.org/10.1143/JJAP.40.4924

[26] Wagner, T., et al., New ag-containing amorphous chalcogenide thin films-prospective materials for rewriteable optical memories. 2001, Pardubice Univ (Czechoslovakia).

[27] Gutwirth, J., T. Wagner, and T. Kohoutek, Mir. Vlcek, S. Schroeter, V. Kovanda, Mil. Vlcek, M. Frumar. Journal of Optoelectronics and Advanced Materials, 2003. 5(5): p. 1139.

[28] Bekheet, A., et al., Applied surface science, 2009. 255(8): p. 4590-4594; https://doi.org/10.1016/j.apsusc.2008.11.080

[29] Adel, G. and A. Abd Rabo, Journal of Ovonic Research, 2009. 5(3).

[30] Dohare, C., N. Mehta, and A. Kumar, Materials chemistry and physics, 2011. 127(1-2): p. 208-213; https://doi.org/10.1016/j.matchemphys.2011.01.067

[31] Dohare, C., M. Imran, and N. Mehta, Journal of Asian Ceramic Societies, 2016. 4(3): p. 252-258; https://doi.org/10.1016/j.jascer.2016.04.003

[32] Abdel-Rahim, M., et al., Journal of Alloys Compounds, 2017. 728: p. 1346-1361; https://doi.org/10.1016/j.jallcom.2017.09.004
[33] Dohare, C. and N. Mehta, Journal of Crystallization Process and Technology, 2012. 2.
[34] Kumar, S., M. Husain, and M. Zulfequar, Physica B: Condensed Matter, 2006. 371(2): p. 193-198; https://doi.org/10.1016/j.physb.2005.09.021
[35] Mehta, N., D. Sharma, and A. Kumar, Physica B: Condensed Matter, 2007. 391(1): p. 108-112; https://doi.org/10.1016/j.physb.2006.09.004
[36] Mishra, M., et al., Progress in Natural Science: Materials International, 2011. 21(1): p. 36-39; https://doi.org/10.1016/S1002-0071(12)60022-7
[37] Naqvi, S.F., et al., Journal of alloys compounds, 2010. 506(2): p. 956-962; https://doi.org/10.1016/j.jallcom.2010.07.128
[38] Shaaban, E., et al., Journal of Materials Science: Materials in Electronics, 2017. 28(18): p. 13379-13390; https://doi.org/10.1007/s10854-017-7175-0
[39] Sharma, J. and S. Kumar, Physica B: Condensed Matter, 2012. 407(3): p. 457-463; https://doi.org/10.1016/j.physb.2011.11.014
[40] Singh, D., S. Kumar, and R. Thangaraj, Journal of non-crystalline solids, 2012. 358(20): p. 2826-2834; https://doi.org/10.1016/j.jnoncrysol.2012.07.006
[41] Singh, D., S. Kumar, and R. Thangaraj, Progress in Natural Science: Materials International, 2012. 22(5): p. 386-391; https://doi.org/10.1016/j.pnsc.2012.05.003
[42] Singh, D., et al., Physica B: Condensed Matter, 2013. 408: p. 119-125; https://doi.org/10.1016/j.physb.2012.09.034
[43] Tiwari, R., et al., Journal of thermal analysis calorimetry, 2005. 82(1): p. 45-49; https://doi.org/10.1007/s10973-005-0839-7
[44] Sakka, S. and J. Mackenzie Journal of Non-Crystalline Solids, 1971. 6(2): p. 145-162; https://doi.org/10.1016/0022-3093(71)90053-6
[45] Šesták, J., Journal of Thermal Analysis Calorimetry, 1988. 33(1): p. 75-85; https://doi.org/10.1007/BF01914586
[46] Yinnon, H. and D.R. Uhlmann, Journal of Non-Crystalline Solids, 1983. 54(3): p. 253-275; https://doi.org/10.1016/0022-3093(83)90069-8
[47] Surinach, S., et al., Journal of materials science, 1984. 19(9): p. 3005-3012; https://doi.org/10.1007/BF01026979
[48] Hu, L. and Z. Jiang, Journal of the Chinese Ceramic Society, 1990. 18(4): p. 315-321.
[49] Kissinger, H.E., Analytical chemistry, 1957. 29(11): p. 1702-1706; https://doi.org/10.1021/ac60131a045
[50] Vazquez, J., et al., Journal of Alloys and Compounds, 2003. 354(1-2): p. 153-158; https://doi.org/10.1016/S0925-8388(02)01364-6
[51] J.C.Phillips and M.F.Thorpe, Solid State Communications, 1985. 53(8): p. 699-702; https://doi.org/10.1016/0038-1098(85)90381-3
[52] Ribes, M., E. Bychkov, and A. Pradel, Journal of Optoelectronics and Advanced Materials, 2001. 3(3): p. 665-674.
[53] Tanaka, K., Physical Review B, 1989. 39(2): p. 1270; https://doi.org/10.1103/PhysRevB.39.1270